

Temperature and Ionic Strength Effects on Some Reactions Involving Sulfate Radical [SO₄⁻(aq)]

Zhen-Chuan Bao[†] and John R. Barker^{*,†,‡}

Departments of Atmospheric, Oceanic, and Space Sciences and Chemistry, University of Michigan, Ann Arbor, Michigan 48109-2143

Received: February 7, 1996; In Final Form: April 2, 1996[⊗]

Sulfate radical anion SO₄⁻ was generated by 248 nm laser flash photolysis of K₂S₂O₈ solutions and monitored by time-resolved multipass absorbance at 454 nm. The 320–520 nm absorption spectrum of SO₄⁻ was unaffected by up to 2 M added HClO₄, under the experimental conditions. Three reactions were investigated: (a) SO₄⁻ + SO₄⁻ → S₂O₈²⁻, (b) SO₄⁻ + H₂O → HSO₄⁻ + OH, and (c) SO₄⁻ + S₂O₈²⁻ → products. Rate constant *k_c* was too slow to be measured, and only an upper limit was determined: *k_c* ≤ 10⁴ M⁻¹ s⁻¹. Arrhenius parameters were determined at low ionic strength over the range 11.8–74.4 °C: 2*k_a*/ε = (4.8 ± 2.0) × 10⁵ exp(-1.7 ± 1.1 kJ mol⁻¹/RT) cm s⁻¹ and *k_b* = (4.7 ± 0.1) × 10³ exp(-15.5 ± 0.6 kJ mol⁻¹/RT) M⁻¹ s⁻¹, where ε is the SO₄⁻ absorption coefficient at 454 nm. At 296 K, the values are in good agreement with literature values: 2*k_a*/ε = (2.5 ± 0.2) × 10⁵ cm s⁻¹ and *k_b*[H₂O] = 440 ± 50 s⁻¹. Rate constants *k_a* and *k_b* were found to increase strongly and nonlinearly with increasing ionic strength (added NaClO₄) or acidity (added HClO₄). Ion-pair formation provides a possible explanation, and a quantitative empirical model is presented for conditions with [Na⁺] ≤ 1.6 M and [H⁺] ≤ 3 M. Using the ion-pair model, estimated ionization equilibrium constants are obtained for the H⁺SO₄⁻ and the Na⁺SO₄⁻ radical ion pairs.

I. Introduction

Free radical reactions in cloud droplets and aerosols have received increased attention in recent years and are now included in some atmospheric chemistry models.^{1–14} In the troposphere, cloud droplets and aerosols which are present as liquid or supercooled liquid can absorb gases and free radicals from the surrounding air mass. Chemical reactions inside the particles can affect not only particle chemical and physical properties but also gas phase chemistry.¹⁵ The rapid oxidation of SO₂ to sulfate observed in the troposphere can only occur in the aqueous phase.¹⁶ Condensed phase reactions can also affect ozone in the troposphere.¹⁷ In the stratosphere, aerosols consist largely of sulfuric acid solutions, which not only have low freezing points, but which can persist as supercooled liquids for long periods.¹⁸ Low temperature, low pH, and high ionic strength are common characteristics of some tropospheric and stratospheric aerosols. Laboratory experimental studies are needed under these extreme conditions to investigate potentially important aqueous phase atmospheric reactions.

Among many potentially important radicals found in cloud droplets and aerosols, SO₄⁻ has a high redox potential and can even oxidize Cl⁻.¹⁹ Investigations of SO₃²⁻(aq) photooxidation implicate the SO₄⁻ radical anion as an important chain carrier in the oxidation of SO₂²⁰ in acid rain chemistry.²¹ However, reactions of SO₄⁻ with other species can reduce the chain length. For accurate atmospheric models, it is important to obtain rate constants of these reactions under atmospheric conditions.

Many SO₄⁻ reaction rate constants have been measured in the laboratory,^{22–37} but few have been measured at low temperature, low pH, or high ionic strength. The aim of this work is to investigate SO₄⁻ reaction kinetics under such conditions. We have determined rate constants for the reactions of SO₄⁻ with SO₄⁻, S₂O₈²⁻, and H₂O in the temperature range

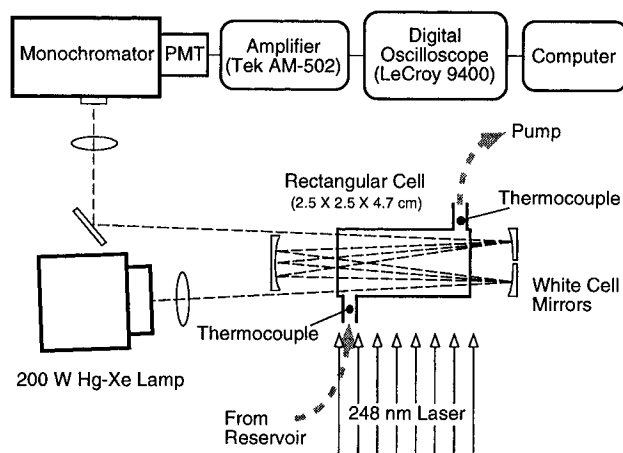


Figure 1. Experimental apparatus. For clarity, not all components are shown.

from 11.8 to 74.4 °C, in the acidity range [H⁺] from ≈ 0 to 3 M, and at ionic strengths ranging from ~10⁻³ to >1.5 M. Not all of these reactions are important in the atmosphere, but all are important in laboratory studies of the atmospheric reactions and therefore must also be understood. Where they can be compared, the rate constants obtained in the present work are generally similar to literature values, although they differ in some details. The measured rate coefficients at high ionic strength and acidity do not obey the Debye–Huckel theory, or its usual extensions, but they can be rationalized quantitatively with an ion-pair model.

II. Experimental Section

The experimental apparatus consists of excimer laser flash photolysis and time-resolved detection of transient species by multipass absorbance (Figure 1). The 248 nm (KrF) excimer laser (Lumonics HyperEx-400) was typically operated at 1.01 Hz with output energy of ~80 mJ per pulse, although other operating conditions were investigated, as described below.

* Address correspondence to this author (jrbarker@umich.edu).

[†] Department of Atmospheric Oceanic, and Space Sciences.

[‡] Department of Chemistry.

[⊗] Abstract published in *Advance ACS Abstracts*, May 15, 1996.

Laser pulse energies were measured with a calorimetric power meter (Scientech). The laser beam was passed without focusing through a rectangular mask, and it illuminated the reaction cell nearly uniformly. The $2.5 \times 2.5 \times 4.7$ cm (~ 29 cm³) rectangular reaction cell was custom-fabricated from Spectrosil far-UV silica by Spectrocell Inc. Reaction mixtures were drawn through the cell by a peristaltic pump (Masterflex Model 7553-70) situated downstream from the cell; flow rates were varied from ~ 0.4 to 5 cm³/s. In experiments with added NaClO₄ or HClO₄, the flow rates were maintained near ~ 0.4 – 0.6 cm³ s⁻¹, while in the other experiments, flows were ~ 5 cm³ s⁻¹. The reaction solutions were not recirculated, and they came in contact only with Pyrex glass and Teflon prior to entering the reaction cell.

Light from a 200 W Hg–Xe arc lamp (Oriel Model 6291) was passed through a lens for collimation, then through a liquid water filter to remove infrared radiation, and finally through a 400 nm cutoff filter (Oriel Filters 51265) to eliminate the UV fraction. A White cell³⁸ with end mirrors of 15 cm radius of curvature was used with 12–16 passes to produce a total absorption pathlength of 60–80 cm. Various apertures and lenses were used to direct the analytical beam and to minimize scattered laser light (for clarity, Figure 1 does not show all details). Light from the White cell was directed to a monochromator (Jarrell-Ash Model NO3) equipped with a photomultiplier tube (Hamamatsu 1P28). The photomultiplier anode current was maintained less than ~ 4 μ A in order to insure linearity of response. Two ~ 400 nm cutoff filters (Oriel Filters 51265 and 51272) were used at the monochromator entrance slit to minimize scattered laser light. The photomultiplier output was terminated by a 1 K Ω resistor; the resulting voltage signal was amplified (Tektronix AM502) and captured with a digital oscilloscope (LeCroy 9400). Signals were averaged for 150–400 laser shots by the oscilloscope and stored on a laboratory computer (Macintosh, Apple Computer) for further analysis. The oscilloscope was triggered by a pyroelectric detector (Moletron Model P3-D1) which monitored the laser pulse. By using the pretrigger feature of the oscilloscope, the transmitted intensity I_0 prior to the pulse was recorded, as well as the time-dependent intensity $I(t)$ following the pulse.

The temperature of the reaction solution was measured at both entrance and exit of the cell by calibrated copper–constantan thermocouples installed in glass thermocouple wells. The average reading from two thermocouples was used to establish the solution temperature. Typically, the two temperatures differed by ≤ 0.5 °C, except at the extreme high and low temperatures of the experiments, where the differences were sometimes as large as 2 °C.

All solutions were freshly prepared immediately before use from the following reagents: K₂S₂O₈ (Fisher), >99.5%, certified; HClO₄ (Fisher), 70%, reagent ACS; NaClO₄ (Aldrich), 98%, ACS reagent. The water used for the preparation of the solutions was purified by a Millipore Milli-Q system, and the resistivity was > 16 M Ω cm.

III. Results and Discussion

1. Chemical Mechanism and Data Analysis. In the present work, the sulfate radical (SO₄⁻) was generated by 248 nm laser flash photolysis of $(1-2) \times 10^{-3}$ M K₂S₂O₈ solutions:^{28,39}



The SO₄⁻ absorption spectrum has a broad absorption band in the visible region with peak absorbance around 450 nm.^{22,24–26,29,32,40–42} Following the laser flash, there is an

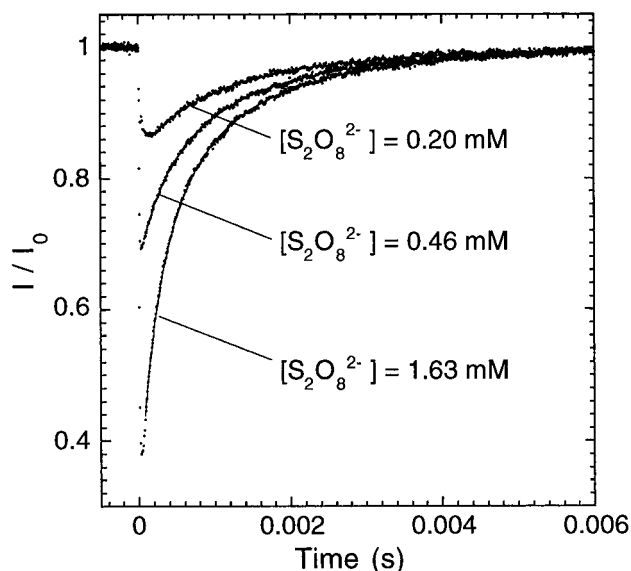
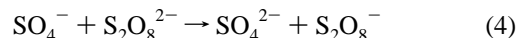
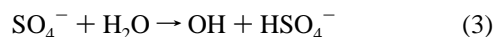


Figure 2. Time-resolved transmittances (points) at room temperature (296 K) for the concentrations shown. Nonlinear least-squares fits are shown as barely visible solid lines through the data.

immediate increase in the absorbance observed at the 454 nm observation wavelength, followed by a decay, as shown in Figure 2. The SO₄⁻ decay kinetics can be described by the following reactions, according to McElroy and Waygood:²⁴



This mechanism predicts that the SO₄⁻ decay is described by mixed first- and second-order kinetics. The time-dependent transmittance of the cell depends on the absorbance $A(t)$ according to the Beer–Lambert equation:

$$\frac{I(t)}{I_0} = \exp(-A(t)) \quad (5)$$

For the mechanism above, the absorbance $A(t)$ can be shown to depend on the sulfate concentration [SO₄⁻] as follows:²⁴

$$A(t) = \epsilon l [\text{SO}_4^{\cdot -}] = \left\{ \exp(C_1 t) \left[\frac{1}{A_0} + \frac{C_2}{C_1 l} \right] - \frac{C_2}{C_1 l} \right\}^{-1} \quad (6)$$

where ϵ is the molar absorption coefficient (base e) of SO₄⁻, l is the optical pathlength, t is time, and $A_0 = \epsilon l [\text{SO}_4^{\cdot -}]_0$ is the initial absorbance (which depends on the initial SO₄⁻ concentration). Nonlinear least-squares fits of eq 6 are also presented in Figure 2, and it is clear that the fits are very good. For the above mechanism, constant C_1 is equal to the pseudo-first-order rate constant:

$$k^1 = k_3[\text{H}_2\text{O}] + k_4[\text{S}_2\text{O}_8^{2-}] \quad (7)$$

where k_3 and k_4 are the rate constants of (3) and (4), respectively. Constant C_2 is given by $C_2 = 2k_2/\epsilon$, where k_2 is the rate constant for (2). By varying experimental conditions and determining constants A_0 , C_1 , and C_2 by nonlinear least-squares fits, it is possible to determine the three rate constants. By varying detection wavelength, it is possible to determine the relative absorption coefficients $\epsilon(\lambda)$ as a function of wavelength. Note

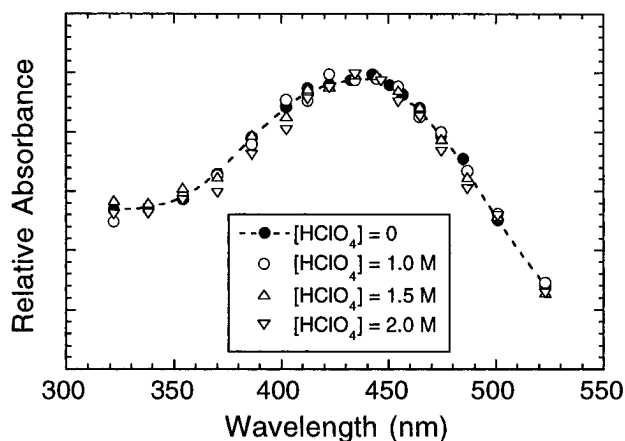


Figure 3. The SO_4^- absorption spectrum at 296 K.

that k_2 cannot be determined independently from the absorption coefficient ϵ . As discussed below, (6) can also be used to fit the data obtained with added NaClO_4 and HClO_4 , but constants C_1 and C_2 take different meanings. The nonlinear least-squares fits were carried out using KaleidaGraph v. 3.0.4 (Abelbeck Software) for Power Macintosh computers. KaleidaGraph utilizes the Marquardt–Levenberg algorithm, and we verified the accuracy of the software by comparison with a well-established code for the algorithm.⁴³

All of the values for C_1 and C_2 presented in the figures are tabulated in Table IS (Supporting Information) along with the experimental conditions for each experiment.

2. The SO_4^- Absorption Spectrum. In the present work, the spectrum of SO_4^- was measured over the range 320–520 nm following 248 nm laser flash photolysis of $\text{K}_2\text{S}_2\text{O}_8$ solutions, and it is shown in Figure 3. In a series of runs, data for $I(t)/I_0$ were fitted as described above and the fitted values for A_0 were obtained. We assumed that $A_0 = \epsilon(\lambda)[\text{SO}_4^-]_0$ and $[\text{SO}_4^-]_0 = \sigma_{248}\phi_{248}[\text{K}_2\text{S}_2\text{O}_8]Q$, where σ_{248} is the absorption cross section of $\text{S}_2\text{O}_8^{2-}$ at 248 nm, ϕ_{248} is the quantum yield for SO_4^- production from $\text{S}_2\text{O}_8^{2-}$ at 248 nm, and Q is the 248 nm laser fluence. According to these assumptions, the absorption cross section is related to measured values of A_0 , $[\text{K}_2\text{S}_2\text{O}_8]$, and Q according to (8):

$$\epsilon(\lambda) \propto \frac{A_0}{[\text{K}_2\text{S}_2\text{O}_8]Q} \quad (8)$$

The relative absorption coefficients agree well with prior work,^{22,24–26,29,32,40–42} except that the absorption peak occurs near 440 nm, rather than 450 nm. When 1, 1.5, and 2 M of perchloric acid (HClO_4) are added to the solution, the observed absolute cross sections remained constant within $\pm 20\%$ (assuming σ_{248} and ϕ_{248} to be independent of added HClO_4). The relative absorption coefficients presented in Figure 3 show little variation as HClO_4 is added, in agreement with other investigations.^{22,26,36} This lack of variation indicates that the protonated sulfate radical (HSO_4^-) has the same spectrum as the sulfate radical anion. Although at first surprising, the SO_4^- radical is not unique in having the same spectrum in ionic and protonated forms: in the carbonate radical system, CO_3^- , and HCO_3^- have virtually identical spectra.⁴⁴

To obtain k_2 from measured values of $2k_2/\epsilon$, a value for the absorption coefficient is required. Recent values for ϵ at 450 nm obtained by other workers are in good agreement.^{3,22,24} For example, Tang *et al.*²² found $\epsilon\phi_{248} = 2770 \pm 280 \text{ M}^{-1} \text{ cm}^{-1}$ and McElroy²³ reported $\epsilon = 1600 \pm 100 \text{ M}^{-1} \text{ s}^{-1}$ (both values are base 10). These are in good agreement, based on $\phi_{248} \approx$

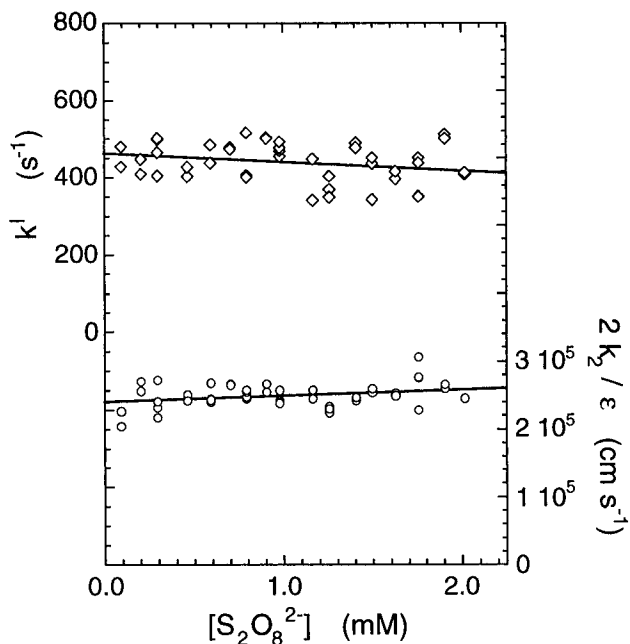


Figure 4. Plots of $2k_2/\epsilon$ and k^1 vs $[\text{S}_2\text{O}_8^{2-}]$ at room temperature (296 K). The solid lines are linear least-squares fits. The small dependences on $[\text{S}_2\text{O}_8^{2-}]$ are not significant (see text).

TABLE 1: Experimental Parameters

parameter	range
laser repetition rate	0.11–19 Hz
laser pulse energy	~9–130 mJ
number of white cell passes	1–16
sample flow rate	~0.5–14 $\text{cm}^3 \text{ s}^{-1}$
probe light intensity (450 nm)	~10 times
$[\text{K}_2\text{S}_2\text{O}_8]$	0.1–2 mM

2.22 In the present work, we have not measured the absolute value of ϵ and we will only report values for $2k_2/\epsilon$, rather than absolute values of k_2 .

3. Experimental Parameters. Experimental parameters such as laser repetition rate, laser pulse energy, analytical light intensity and sample flow rate may affect the observed reaction rates, due to accumulation of reaction products in the cell and multiphoton effects. Signal averaging is used to improve the signal/noise ratio in the present experiments and thus many laser pulses are needed. However, if the cell is completely emptied and refilled between laser shots, large volumes of solution are consumed. Thus it is particularly important to determine whether the results depend on laser pulse repetition frequency and solution flow rate. No such dependence was observed. Table 1 lists experimental parameters that were investigated; the experimental results showed no systematic dependence on any of these parameters within the ranges investigated.

4. Rate Constant Determinations. Three typical SO_4^- time-resolved transmission profiles observed after 248 nm laser flash photolysis of aqueous $\text{S}_2\text{O}_8^{2-}$ solution are shown in Figure 2. Because the pseudo-first-order rate constant k^1 depends on $[\text{S}_2\text{O}_8^{2-}]$ according to (7), we carried out experiments with $[\text{S}_2\text{O}_8^{2-}]$ ranging from 1×10^{-4} to $2 \times 10^{-3} \text{ M}$ at two temperatures (296 and 321 K). The results obtained at 296 K are presented as plots of $2k_2/\epsilon$ and k^1 vs $[\text{S}_2\text{O}_8^{2-}]$ in Figure 4; the results obtained at 321 K are qualitatively similar. The minor dependences of the rate coefficients on $[\text{S}_2\text{O}_8^{2-}]$ are probably due to correlations between C_1 and C_2 in the nonlinear least squares analysis and are not physically significant. This conclusion is consistent with the nonphysical decrease in k^1 as $[\text{S}_2\text{O}_8^{2-}]$ is increased. That neither rate constant varies significantly with $[\text{S}_2\text{O}_8^{2-}]$ is in contrast with the results for k^1 reported

TABLE 2: Recent Data on Sulfate Radical Reactions Near 300 K

SO ₄ ⁻ source ^a	pH	μ (mM)	k ^l (s ⁻¹)	2k ₂ /ε (10 ⁵ cm s ⁻¹)	reference
S ₂ O ₈ ²⁻ LFP (193 nm)		0.3–3	not considered	5.6 ^b	Huie <i>et al.</i> (1989, 1993)
S ₂ O ₈ ²⁻ LFP (248 nm)	1.5–5.4	1.5–410	360 ± 90	3.9 ± 1.1 (at μ = 0)	Tang <i>et al.</i> (1988)
S ₂ O ₈ ²⁻ LFP (248 nm)	4.9–5.2	0.75–8.3	500 ± 60	5.5 ± 0.2 (at μ = 0)	McElroy and Waygood (1990)
H ₂ SO ₄ PR	concd acid	concd acid	500 (assumed)	9.5 (at all [H ⁺])	Jiang <i>et al.</i> (1992)
S ₂ O ₈ ²⁻ LFP (248 nm)	5	not reported	660 ± 40	2.3 ± 0.6 ^b	Herrmann <i>et al.</i> (1995)
S ₂ O ₈ ²⁻ LFP (248 nm)	4.8–5.8	0.28–6.1	440 ± 50	2.5 ± 0.2 (μ ≈ 0)	this work

^a LFP = laser flash photolysis; PR = pulse radiolysis. ^b Obtained by dividing a reported rate constant by ε/2 = 1385/2 M⁻¹ cm⁻¹.

TABLE 3: Differences Due to Fitting Method

	fit I(t)/I ₀ vs time	fit A(t) vs time
k ^l (s ⁻¹)	440	442
2k ₂ /ε (10 ⁵ cm s ⁻¹)	2.5	3.4

by McElroy *et al.*²⁴ and Herrmann *et al.*,³⁷ but it is in agreement with the results of Tang *et al.*²² From our results, we estimate that the upper limit to the rate of (4) is k₄ ≤ 10⁴ M⁻¹ s⁻¹.

At 296 K, the average values obtained for 2k₂/ε and k^l are (2.5 ± 0.2) × 10⁵ cm s⁻¹ and 440 ± 50 s⁻¹, respectively, where the ±1σ errors represent precision only. Our results are compared with those from other recent investigations in Table 2, where it is apparent that our results for 2k₂/ε tend to fall near the lower end of the range. One possible reason for the range of reported rate constants is because least squares fitting of I(t)/I₀ instead of A(t) gives systematically different results. In the experiments, I(t) and I₀ were measured directly; transforming them to A(t) by taking the logarithm of I(t)/I₀ requires that the data be weighted unequally when carrying out the least-squares analysis. If the change in weighting is neglected in the least-squares analysis, the accuracy of the results can be affected. As a test of this effect, we repeated the least-squares analysis for several runs, but fitted A(t) vs t, rather than I(t)/I₀ vs t. The results are listed in Table 3, and it is clear that fitting A(t) produces significantly larger values for 2k₂/ε, while k^l is affected only slightly. The magnitude of this difference is the same as the difference between our results for 2k₂/ε and those of Tang *et al.*²² Since directly fitting I(t)/I₀ vs t with equally weighted data is the proper procedure, all of the rate constants reported in this work were obtained by that method.

The reduction potential for the SO₄⁻/SO₄²⁻ couple can be determined from our result for k₃ and results obtained by Tang *et al.*²² for the reverse reaction, which can be neglected under our conditions, because [HSO₄⁻] is negligible. From the present work, k₃ = k^l/[H₂O] = 7.9 M⁻¹ s⁻¹ and from Tang *et al.*,²² k₋₃ = 3.5 × 10⁵ M⁻¹ s⁻¹. Thus the equilibrium constant K₃ is

$$K_3 = \frac{k_3}{k_{-3}} = 2.26 \times 10^{-5} \quad (9)$$

which is related to the reduction potential difference ΔE₃^o between the couples by the expression⁴⁵

$$\Delta E_3^o / \text{mV} \approx 59.1 \log K_3 \quad (10)$$

where

$$\Delta E_3^o = E^o(\text{SO}_4^- / \text{SO}_4^{2-}) - E^o(\text{H}^+, \text{OH}) / \text{H}_2\text{O} \quad (11)$$

If we take E^o(H⁺, OH)/H₂O = 2.72 V,⁴⁶ we find E^o(SO₄⁻/SO₄²⁻) = 2.45 V, which is in very good agreement with a recommended value: 2.43 V.⁴⁷

5. Temperature Dependence. Although (2) and (3) have been studied previously in several investigations at room temperature, only one temperature-dependent measurement has been performed for (2)⁴⁸ and for (3).³⁷ We carried out experiments

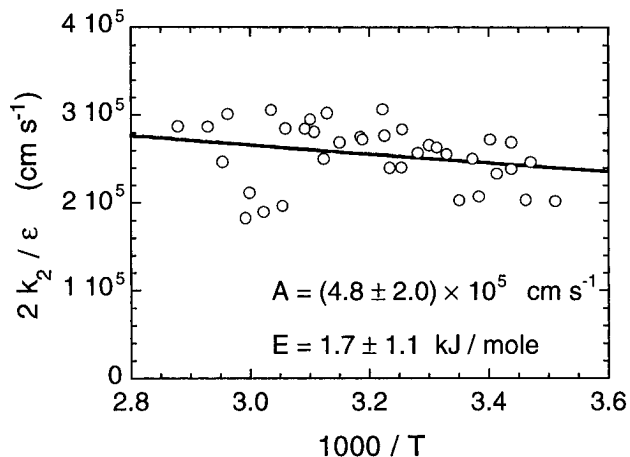


Figure 5. Arrhenius plot of 2k₂/ε (points) and nonlinear least-squares fit (line).

over the range 11.8–74.4 °C, and the results are presented in Figures 5 and 6. Nonlinear least-squares fits gave the following Arrhenius expressions:

$$2k_2/\epsilon = (4.8 \pm 2.0) \times 10^5 \exp(-1.7 \pm 1.1 \text{ kJ mol}^{-1}/RT) \text{ cm s}^{-1} \quad (12)$$

$$k^l = (2.6 \pm 0.6) \times 10^5 \exp(-15.5 \pm 0.6 \text{ kJ mol}^{-1}/RT) \text{ s}^{-1} \quad (13)$$

$$k_3 = (4.7 \pm 0.1) \times 10^3 \exp(-15.5 \pm 0.6 \text{ kJ mol}^{-1}/RT) \text{ M}^{-1} \text{ s}^{-1} \quad (14)$$

where k^l has been identified with k₃[H₂O] and the uncertainties are ±1σ statistical errors. The rate constant for (2) is nearly independent of temperature, in agreement with the results obtained by Huie *et al.*⁴⁸ The activation energy for (3) is consistent with the fact that the reaction is endothermic. The values obtained in the present work for k₃ are in fair agreement with those reported by Herrmann *et al.*,³⁷ but both the activation energy and A factor differ significantly. The reason for this difference cannot be determined, because no experimental details or actual experimental results are described in that report.³⁷

6. pH and Ionic Strength Dependence. In concentrated solutions, the ionic strength is an important parameter, because each ion is surrounded by an extended solvation shell which can affect ionic activities and rate constants. The influence of ionic strength on reaction rate constants k₂ and k₃ has been investigated previously for μ ≤ 0.4.^{22,24} In the present work, we carried out systematic experiments at ionic strengths up to >1.5 M by adding NaClO₄ to the K₂S₂O₈ solutions. At NaClO₄ concentrations greater than ~2 M, the results were not reproducible when different batches of reagent were used, probably due to the presence of impurities. Impurities may also be responsible for the appearance of tiny suspended particles,

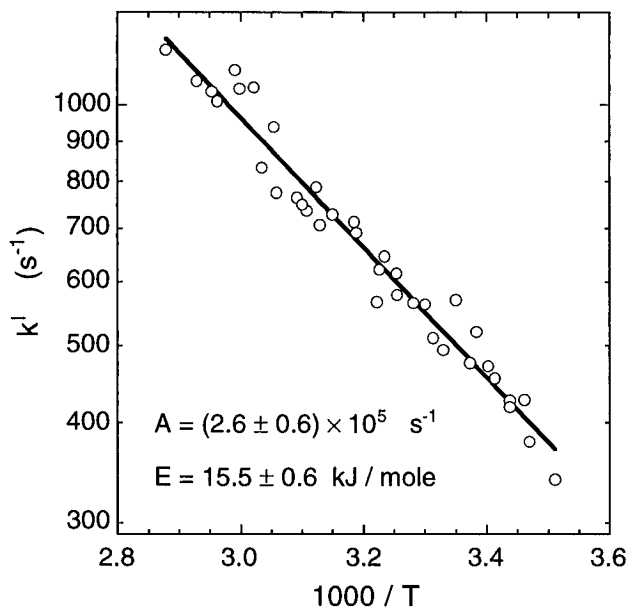


Figure 6. Arrhenius plot of k^1 (points) and nonlinear least-squares fit (line).

which scattered the laser light, at high NaClO_4 concentrations. Thus we report only the results up to ~ 2 M of NaClO_4 ($\mu \approx 1.6$ M) where the results were reproducible.

At relatively low ionic strengths, transition state theory can be combined with the Debye–Huckel (DH) theory and an empirical term ($-b\mu$) introduced by Davies to obtain the Debye–Huckel–Bronsted–Davies (DHBD) equation:⁴⁹

$$\log k = \log k^\circ + 2Z_A Z_B A \left\{ \frac{\mu^{1/2}}{1 + \mu^{1/2}} \right\} - b\mu \quad (15)$$

where k is the observed rate constant, k° is the rate constant at infinite dilution, A is the Debye–Huckel constant ($A = 0.509$ at 298 K), Z_A and Z_B are charges for species A and B, respectively, μ is the total ionic strength, and b is an empirical parameter. Equation 15 predicts an increase of k with increasing ionic strength for the reaction between two ions of like sign. For a few reaction systems for which data are available, (15) with $b \approx 0.2$ – 0.3 is reasonably accurate up to moderate ionic strengths ($\mu < 0.5$).⁵⁰ Note that the activity coefficient of an ion does not monotonically approach zero as the ionic strength increases, but it can increase again for large μ , because the amount of solvent available for solvation of ions decreases as μ increases; decreasing the amount of water tends to reduce solvation screening and the ions become more active.⁵¹

If one of the reactants is a neutral molecule, then $Z_B = 0$ in (15) and the rate constant depends on the empirical linear term.⁵² At higher ion concentrations, higher order terms may become important, but usually only the linear term is retained:

$$\log k = \log k^\circ - b'\mu \quad (16)$$

where b' is an empirical constant which depends on the difference between the activities of the reactants and that of the transition state: not even its sign can be predicted.⁵³

Plots of some of the data for $2k_2/\epsilon$ and k_3 as functions of $\mu^{1/2}/(1 + \mu^{1/2})$ and μ , respectively, at 296 K are presented in Figures 7 and 8, where it is clear that both $2k_2/\epsilon$ and k_3 increase with increasing ionic strength. The results for $2k_2/\epsilon$ are in reasonable agreement with those obtained by Tang *et al.*²² (aside from the differences in least-squares fitting discussed above), and they can be fitted by the DHBD equation (15), as shown in Figure 7. In sharp contrast, the plot of $k_3[\text{H}_2\text{O}]$ vs μ shown in

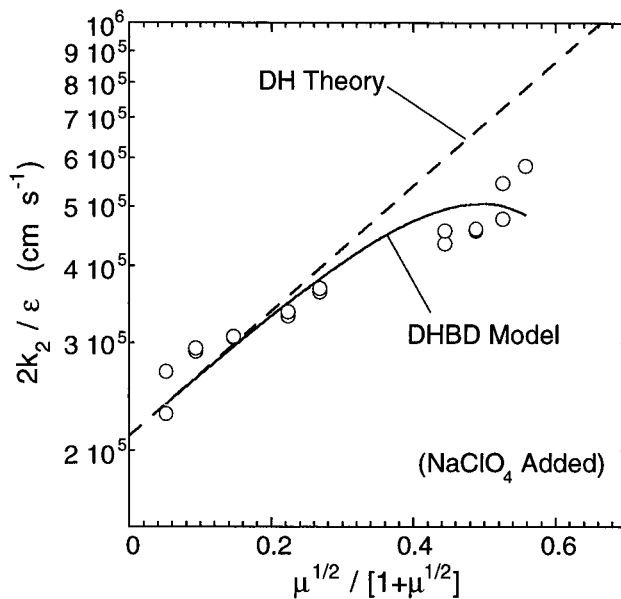


Figure 7. Ionic strength dependence of $2k_2/\epsilon$ at 296 K; the solid line is a least-squares fit of the experimental data to the DHBD equation. The Debye–Huckel (DH) theory limiting slope is shown for comparison (broken line). The ionic strength was varied by adding NaClO_4 .

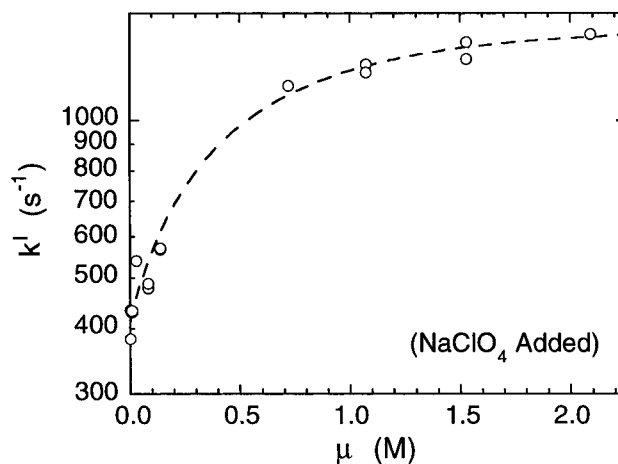


Figure 8. Ionic strength dependence of k^1 ; the broken line is merely intended to guide the eye. The ionic strength was varied by adding NaClO_4 .

Figure 8 is totally inconsistent with (16), which predicts a straight line. Higher order empirical terms could be added to (16) to account for the strong “saturation” behavior, but they provide no further insight. We find it more satisfactory to seek a physical explanation for the observed behavior. The ion-pair mechanism described below provides such an explanation and gives a self-consistent description of all of our experimental data.

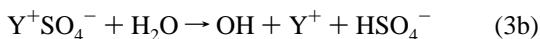
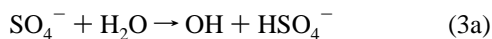
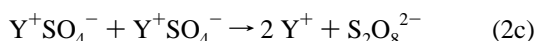
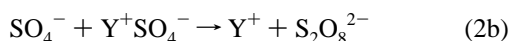
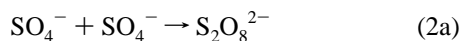
The concept of ion-pair formation was introduced by Bjerrum in order to explain the strong nonlinear dependence of some reaction rate constants on ionic strength.⁵⁴ He proposed that the Coulombic attraction between ions of opposite charge could, to some extent, overcome the thermal energy that tends to separate ions after they have been hydrated in aqueous solutions. Later workers invoked ion-pair formation to explain the numerous deviations of reaction rates from the Debye–Huckel theory in studies of salt effects.^{55–63} Davies⁶⁴ pointed out that ion association can modify the reaction in two ways: firstly, ion pair formation affects the total ionic strength of the medium; secondly, one (or more) such ion pairs may be involved in the

rate-determining step, thus altering the charge of the activated complex and reaction rate.

In the present work, large excesses of NaClO₄ or HClO₄ were added to K₂S₂O₈ solutions. Neutral ion pairs (e.g. K⁺SO₄⁻, Na⁺SO₄⁻, and H⁺SO₄⁻) can coexist in equilibrium with single ions (e.g. SO₄⁻, K⁺, Na⁺, etc.). It is possible that these ion pairs react even more rapidly than the single ions, because of the reduction in the charge of the activated complex.⁶⁴ The higher their charge and the smaller their radius in solution, the more efficient the cations become in accelerating the rate of reaction between ions of like sign.⁴⁹ Reactions between an ion and a neutral ion pair can also have a larger rate constant than that for the reaction between two ions.

When NaClO₄ is in great excess, low concentration species (e.g. K⁺, SO₄⁻, S₂O₈²⁻, K⁺SO₄⁻, Na⁺SO₄⁻, and H⁺SO₄⁻) contribute little to the total ionic strength, compared with Na⁺, ClO₄⁻, and the ion pair Na⁺ClO₄⁻. The Na⁺ClO₄⁻ association constant is $K \approx 0.2 \text{ M}^{-1}$ at room temperature,⁶⁵ but the dependence of this association constant on ionic strength is not known. In order to calculate the total ionic strength, we neglected the minor species and assumed $K = 0.2 \text{ M}^{-1}$ for Na⁺ClO₄⁻ at all μ .

A mechanism incorporating sulfate radical ion pairing can be written by neglecting possible ion complexes containing more than one cation.⁵² In the following reaction scheme, Y = Na or H:



For the Y⁺SO₄⁻ radical ion pair, there is an association constant $K_Y = [\text{Y}^+\text{SO}_4^-]/[\text{Y}^+][\text{SO}_4^-]$, and we assume that this equilibrium is maintained at all times. The differential equations for this reaction set can be integrated and the result is the same as (6), except that constants C₁ and C₂ take the following meanings:

$$C_1 = \{\epsilon_e(K_Y[\text{Y}^+] + 1)\}^{-1} \{\epsilon_i k_{3a} + \epsilon_{ip} k_{3b} K_Y[\text{Y}^+]\} \quad (17)$$

$$C_2 = \{\epsilon_e(K_Y[\text{Y}^+] + 1)\}^{-2} \times \{2\epsilon_i k_{2a} + (\epsilon_i + \epsilon_{ip}) k_{2b} K_Y[\text{Y}^+] + 2\epsilon_{ip} k_{2c} K_Y^2[\text{Y}^+]^2\} \quad (18)$$

where ϵ_i and ϵ_{ip} are the absorption coefficients for SO₄⁻ and Y⁺SO₄⁻, respectively, and ϵ_e is given by the following expression:

$$\epsilon_e = \frac{\epsilon_i}{(1 + K_Y[\text{Y}^+])} + \frac{\epsilon_{ip} K_Y[\text{Y}^+]}{(1 + K_Y[\text{Y}^+])} \quad (19)$$

In the present system, these expressions simplify, because the absorption spectrum does not depend on [H⁺] and [Na⁺]; therefore $\epsilon_i = \epsilon_{ip}$. Rate constant k_{2a} is probably the most dependent on μ , because it involves two anions; the others involve an ion and a neutral, or two neutrals. Therefore, we assumed that k_{2a} obeys (15) with $b = 0.3$, but the other individual rate coefficients are independent of μ .

The experimental results obtained using added NaClO₄ and HClO₄ are consistent with this ion pair model, as shown in

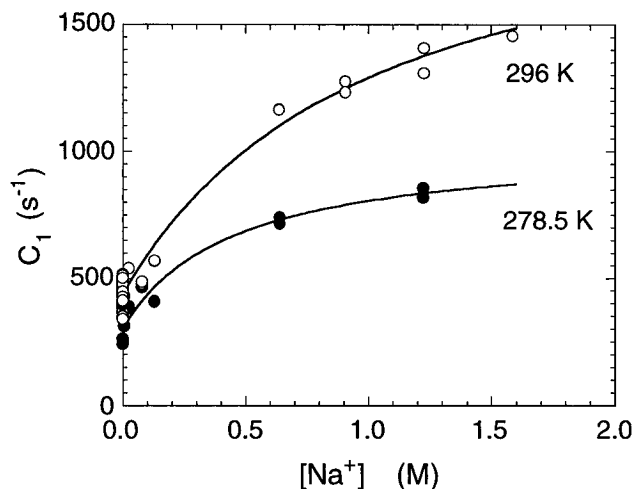


Figure 9. Constant C₁ vs [Na⁺] (points) and least-squares fits according to the ion pair mechanism (lines) at two temperatures. See text for details.

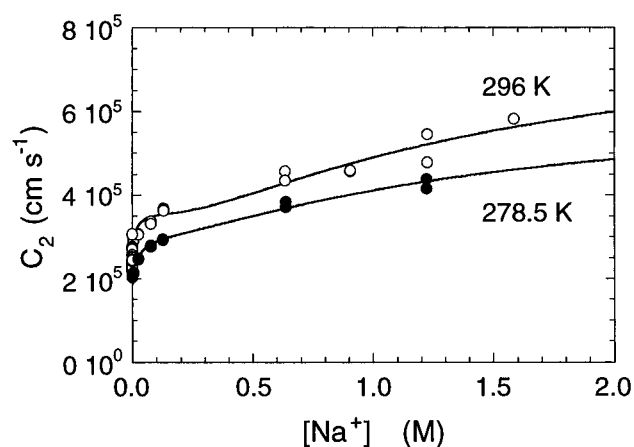


Figure 10. Constant C₂ vs [Na⁺] (points) and least-squares fits according to the ion pair mechanism (lines) at two temperatures. See text for details.

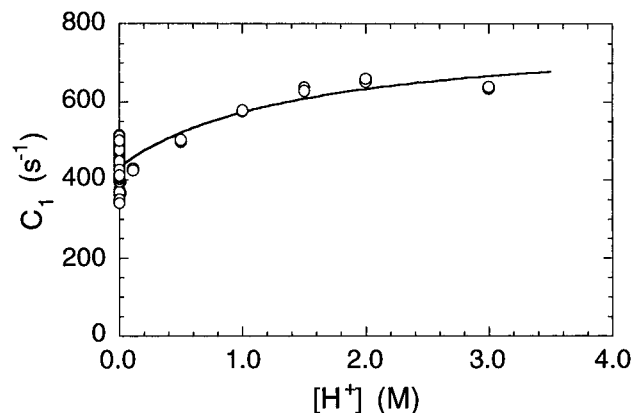
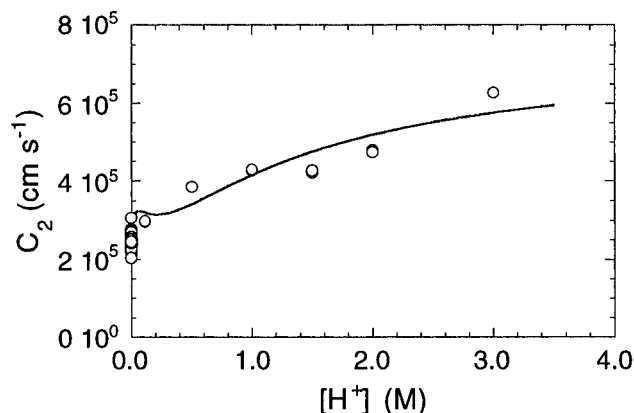


Figure 11. Constant C₁ vs [H⁺] (points) and least-squares fit according to the ion pair mechanism (line) at 296 K. See text for details.

Figures 9–12, where the data were least-squares fitted to (6) to obtain values of C₁ and C₂. In Figures 9 and 11, the solid lines were obtained from nonlinear least-squares fits of C₁ as functions of [Na⁺] and [H⁺], respectively, according to (17) to obtain values of k_{3a} , k_{3b} , and K_Y (for Y = Na, H). We then used the resulting values of K_Y in (18) and carried out least-squares fits of C₂ as functions of [Na⁺] and [H⁺], in order to determine the remaining rate coefficients. The least-squares fits included the ionic strength dependence of k_{2a} , as described

TABLE 4: Parameters for Ion-Pair Mechanism

	Y = Na ⁺ (296 K)	Y = Na ⁺ (278.5 K)	Y = H ⁺ (296 K)
$K_Y = [\text{YSO}_4]/[\text{Y}^+][\text{SO}_4^-] \text{ (M}^{-1}\text{)}$	0.99 ± 0.25	2.2 ± 0.8	0.7 ± 0.5
$(2\epsilon_i/\epsilon_c^2)k_{2a}^\circ \text{ (10}^5 \text{ cm s}^{-1}\text{)}$	2.48 ± 0.02	1.86 ± 0.04	2.42 ± 0.03
$((\epsilon_i + \epsilon_{ip})/\epsilon_c^2)k_{2b} \text{ (10}^5 \text{ cm s}^{-1}\text{)}$	2.5 ± 0.8	3.5 ± 0.5	1.9 ± 0.8
$(2\epsilon_{ip}/\epsilon_c^2)k_{2c} \text{ (10}^5 \text{ cm s}^{-1}\text{)}$	12.8 ± 0.8	6.4 ± 0.3	12.5 ± 0.7
$(\epsilon_i/\epsilon_c)k_{3a} \text{ [H}_2\text{O] (s}^{-1}\text{)}$	436 ± 7	302 ± 20	432 ± 7
$(\epsilon_{ip}/\epsilon_c)k_{3b} \text{ [H}_2\text{O] (s}^{-1}\text{)}$	2150 ± 215	1030 ± 97	781 ± 124

**Figure 12.** Constant C_2 vs $[\text{H}^+]$ (points) and least-squares fit according to the ion pair mechanism (line) at 296 K. See text for details.

above. The parameters extracted from this analysis are summarized in Table 4.

First, consider the association equilibrium constants. Davies⁵² observed that for inorganic salts a decrease of one unit of negative charge leads to a decrease by about a factor of 10 in the association equilibrium constant, as long as the ionic size remains constant. The NaSO_4^- association constant⁵² at 296 K is about $K \approx 5 \text{ M}^{-1}$ and that for the Na^+SO_4^- association was found in the present work to be about $0.99 \pm 0.25 \text{ M}^{-1}$ (see Table 4), in reasonable agreement with Davies' observation.

For the HSO_4^- ion, the association constant is about $K \approx 10^2 \text{ M}^{-1}$,⁴⁹ while that for the H^+SO_4^- ion pair was found in the present work to be $0.7 \pm 0.5 \text{ M}^{-1}$ (Table 4). The ratio of the two association constants is greater than predicted by Davies, but it is consistent with a suggestion by Jiang *et al.*³⁶ that this equilibrium be compared with that of the isoelectronic phosphate radical and some other structurally similar radicals. All of the radicals listed by Jiang *et al.* are much stronger acids than their parent species, and the association constant ratios are often of the order of 10^2 , similar to the $\text{HSO}_4^-/\text{H}^+\text{SO}_4^-$ comparison.

It is difficult to determine whether the fitted rate coefficients for (2a)–(2c) are reasonable. The fitted results for (2a) in the limit of $\mu = 0$ are quite consistent with the results obtained above for $\mu \approx 0$, but this is expected, since the $\mu \approx 0$ data are included in the least-squares fits. For $Y = \text{Na}$, rate constant k_{2b} , which is assumed to have no dependence on μ , is in close agreement with the k_{2a}° result, while rate constant k_{2c} is 3–5 times as large, in general agreement with the conclusion that a larger rate coefficient is expected when the charge of the transition state is reduced, as mentioned above. For $Y = \text{H}$, however, rate constant k_{2b} is less than k_{2a}° , the reverse of the expected trend. Considering the large uncertainty in k_{2b} , however, this inconsistency is not serious.

The nonmonotonic behavior exhibited by C_2 in Figures 10 and 12 comes directly from the nonlinear least-squares fits and is due to the changing composition of the solutions as $Y^+ = \text{Na}^+, \text{H}^+$ concentrations are varied. At higher $[\text{Y}^+]$, the ion-pair concentrations increase and the simple ion concentrations decrease. These changes cause C_2 to depend more on k_{2b} and k_{2c} than on k_{2a} at high $[\text{Y}^+]$. Rate constants k_{2a} and k_{2b} are

much smaller than k_{2c} , however, and this difference produces the “kinks” in the plots.

The ion-pair model and the rate constants summarized in Table 4 provide a complete quantitative description of the reaction system for $[\text{Na}^+] \leq 1.6 \text{ M}$ and $[\text{H}^+] \leq 3 \text{ M}$. Although the kinetics evidence indicates an ion-pair mechanism is operative, this conclusion has not been investigated with other independent measurements. The assumed reaction model is consistent with the experimental kinetics data, but these data may be consistent with other models, as well. The present mechanism provides a good description of the experimental results, but it is not necessarily correct. Moreover, the least-squares fits of these rate coefficients are somewhat statistically correlated and they depend on the equilibrium constant, which is itself somewhat uncertain. In light of these considerations, the numerical rate constants and equilibrium constants are only applicable within the experimental range of the present investigation and should not be used for extrapolations outside this range.

IV. Atmospheric Implications

Because of the relatively low concentration of SO_4^- generated in the atmospheric condensed phase, (2) is probably not important and need not be included in atmospheric chemistry models. This eliminates the need to consider many of the complexities of the ion-pair mechanism in atmospheric models. In laboratory studies, however, (2) is very important and must be included in a complete mechanism. Since liquid water is usually present in the atmospheric condensed phase, (3) can be important and it is included in a model developed by Jacob *et al.*,⁶⁶ although with an incorrect estimate for the activation energy, which has been measured in the present work.

An important feature of the present work is use of the ion-pair model to explain the rate constant dependences on pH and ionic strength. The present work cannot prove or disprove the ion-pair model, but if it is correct, it can be a very useful tool in modeling high-concentration environments, such as occur in stratospheric aerosols, which are composed principally of 70–80 wt % sulfuric acid with traces of a variety of other compounds,⁶⁷ and in sea salt aerosols, which contain highly concentrated NaCl solutions. In future work, we will investigate reactions in such environments. Since rate coefficients depend strongly and unpredictably on the ionic strength, much further work remains to be done.

Acknowledgment. We thank NASA for financial support under the auspices of the Atmospheric Effects of Aviation/Subsonic Assessment Program. We also thank Dr. Paul Wine and Dr. Robert Huie for very helpful conversations and suggestions regarding experimental details.

Supporting Information Available: Measured parameters and experimental conditions for all the data presented in the figures (Table IS) (6 pages). Ordering information is given on any current masthead page.

References and Notes

- (1) Chameides, W. L.; Davis, D. D. *J. Geophys. Res., D: Atmos.* **1982**, *87*, 4863.

- (2) Graedel, T. E.; Goldberg, K. I. *J. Geophys. Res., D: Atmos.* **1983**, *88*, 10865.
- (3) Chameides, W. L. *J. Geophys. Res., D: Atmos.* **1984**, *89*, 4739.
- (4) Jacob, D. J. *J. Geophys. Res., D: Atmos.* **1986**, *91*, 9807.
- (5) Jacob, D. J.; Gottlieb, E. W.; Prather, M. J. *J. Geophys. Res., D: Atmos.* **1989**, *94*, 12975.
- (6) Heikes, B. G.; Thompson, A. M. *J. Geophys. Res., D: Atmos.* **1983**, *88*, 10883.
- (7) Lelieveld, J.; Crutzen, P. J. *Nature* **1990**, *343*, 227.
- (8) Dentener, F. J.; Crutzen, P. J. *J. Geophys. Res., D: Atmos.* **1993**, *98*, 7149.
- (9) Warneck, P. *Fresenius J. Anal. Chem.* **1991**, *340*, 585.
- (10) Warneck, P. *Ber. Bunsenges. Phys. Chem.* **1992**, *96*, 454.
- (11) Graedel, T. E.; Weschler, C. J. *Rev. Geophys. Space Phys.* **1981**, *19*, 505.
- (12) Chameides, W. L.; Stelson, A. W. *Ber. Bunsenges. Phys. Chem.* **1992**, *96*, 461.
- (13) Colville, R. N.; Sander, R.; Choularton, T. W.; Bower, K. N.; Inglis, D. W. F.; Wobrock, W.; Schell, D.; Svenningsson, I. B.; Wiedensohler, A.; Hansson, H.-C.; Hallberg, A.; Ogren, J. A.; Noone, K. J.; Facchini, M. C.; Fuzzi, S.; Orsi, G.; Arends, B. G.; Winiwarter, W.; Schneider, T.; Berner, A. *J. Atmos. Chem.* **1994**, *19*, 189.
- (14) Sander, R.; Lelieveld, J.; Crutzen, P. J. *J. Atmos. Chem.* **1995**, *20*, 89.
- (15) Kolb, C. E.; Worsnop, D. R.; Zahniser, M. S.; Davidovits, P.; Keyser, L. F.; Leu, M.-T.; Molina, M. J.; Hanson, D. R.; Ravishankara, A. R.; Williams, L. R.; Tolbert, M. A. *Problems and Progress in Atmospheric Chemistry*; Barker, J. R., Ed.; World Scientific publishing Co.: Singapore, 1995; p 771.
- (16) Warneck, P. *Chemistry of the Natural Atmosphere*; Academic Press, Inc.: San Diego, 1988.
- (17) Lelieveld, J.; Crutzen, P. J. *Nature* **1990**, *343*, 227.
- (18) Dye, J. E.; Baumgardner, D.; Gandrud, B. W.; Kawa, S. R.; Kelly, K. K.; Loewenstein, M.; Ferry, G. V.; Chan, K. R.; Gary, B. L. *J. Geophys. Res.* **1992**, *97*, 8015.
- (19) Huie, R. E. *Problems and Progress in Atmospheric Chemistry*; Barker, J. R., Ed.; World Scientific publishing Co.: Singapore, 1995; p 374.
- (20) Deister, U.; Warneck, P. *J. Phys. Chem.* **1990**, *94*, 2191.
- (21) Scire, J. A.; Venkatram, A. *Atmos. Environ.* **1985**, *19*, 637.
- (22) Tang, Y.; Thorn, R. P.; Mauldin, R. L.; Wine, P. H. *J. Photochem. Photobiol. A* **1988**, *44*, 243.
- (23) McElroy, W. J. *J. Phys. Chem.* **1990**, *94*, 2435.
- (24) McElroy, W. J.; Waygood, S. J. *J. Chem. Soc., Faraday Trans.* **1990**, *86* (14), 2557.
- (25) Heckel, V. E.; Henglein, A.; Beck, G. *Ber. Bunsenges. Phys. Chem.* **1966**, *70*, 149.
- (26) Dogliotti, L.; Hayon, E. *J. Phys. Chem.* **1967**, *71*, 2511.
- (27) Dogliotti, L.; Hayon, E. *J. Phys. Chem.* **1967**, *71*, 3802.
- (28) Kraljic, I. *Int. J. Radiat. Phys. Chem.* **1970**, *2*, 59.
- (29) Hayon, E.; Treinin, A.; Wilf, J. *J. Am. Chem. Soc.* **1972**, *94*, 47.
- (30) Redpath, J. L.; Willson, R. L. *Int. J. Radiat. Biol.* **1975**, *27*, 389.
- (31) Chawla, O. P.; Fessenden, R. W. *J. Phys. Chem.* **1975**, *79*, 2693.
- (32) Kim, K. J.; Hamill, W. H. *J. Phys. Chem.* **1976**, *80*, 2320.
- (33) Maruthamuthu, P.; Neta, P. *J. Phys. Chem.* **1978**, *82*, 710.
- (34) Eibenberger, H.; Steenken, S.; Neill, P. O. *J. Phys. Chem.* **1978**, *82*, 749.
- (35) Huie, R. E.; Neta, P. *Atmos. Environ.* **1987**, *21*, 1743.
- (36) Jiang, P. Y.; Katsumura, Y.; Nagaishi, R.; Domae, M.; Ishikawa, K.; Ishiguro, K. *J. Chem. Soc., Faraday Trans.* **1992**, *88* (12), 1653.
- (37) Herrmann, H.; Reese, A.; Zellner, R. *J. Mol. Struct.* **1995**, *348*, 183.
- (38) White, J. U. *J. Opt. Soc. Am.* **1942**, *32*, 285.
- (39) Hayon, E.; McGarvey, J. J. *J. Phys. Chem.* **1967**, *71*, 1472.
- (40) hayon, E.; McGarvey, J. J. *J. Phys. Chem.* **1967**, *71*, 1472.
- (41) Robke, W.; Renz, M.; Henglein, A. *Int. J. Radiat. Phys. Chem.* **1969**, *1*, 39.
- (42) Lesigue, B.; Ferradini, C.; Pucheault, J. *J. Phys. Chem.* **1973**, *77*, 2156.
- (43) Bevington, P. R. *Data Reduction and Error Analysis for the Physical Sciences*; McGraw-Hill: New York, 1969; Chapter 11.
- (44) Chen, S.-N.; Cope, V. W.; Hoffman, M. Z. *J. Phys. Chem.* **1973**, *77* (9), 1111.
- (45) Wardman, P. *J. Phys. Chem. Ref. Data* **1989**, *18* (4), 1639.
- (46) Stanbury, D. M. *Adv. Inorg. Chem.* **1989**, *33*, 75.
- (47) Huie, R. E.; Clifton, C. L.; Neta, P. *Radiat. Phys. Chem.* **1991**, *38* (5), 477.
- (48) Huie, R. E.; Clifton, C. L. *Chem. Phys. Lett.* **1993**, *205* (2, 3), 163.
- (49) Perlmutter-Hayman, B. *Progr. React. Kin.* **1971**, *6*, 239.
- (50) Pankow, J. F. *Aquatic Chemistry Concepts*; Lewis Publishers: Boca Raton, FL, 1991; p 48.
- (51) Bockris, J. O'M.; Reddy, A. K. N. *Modern Electrochemistry*; Plenum Press: New York, 1970, Vol. 1, p 238.
- (52) Davies, C. W. *Ion Association*; Butterworths: North Ryde, Australia, 1962.
- (53) Moore, J. W.; Pearson, R. G. *Kinetics and Mechanism*; John Wiley & Sons: New York, 1981; p 272.
- (54) Bjerrum, N. K. *Dan. Vidensk. Selsk.* **1926**, *7*, 1.
- (55) Bronsted, J. N.; Livingston, R. *J. Am. Chem. Soc.* **1927**, *49*, 435.
- (56) Olson, A. R.; Simonson, T. R. *J. Chem. Phys.* **1947**, *17*, 1167.
- (57) Bell, R. P.; Prue, J. E. *J. Chem. Soc.* **1949**, 362.
- (58) Lamer, V. K. *J. Am. Chem. Soc.* **1929**, *51*, 3341, 3678.
- (59) King, C. V.; Jacobs, M. B. *J. Am. Chem. Soc.* **1931**, *53*, 1704.
- (60) Howells, W. J. *J. Chem. Soc.* **1939**, 463.
- (61) Indelli, A.; Prue, J. E. *J. Chem. Soc.* **1959**, 107.
- (62) Bronsted, J. N.; Delbanco, A. *Z. Anorg. Chem.* **1925**, *144*, 248.
- (63) Holmberg, B. *Z. Phys. Chem.* **1913**, *81*, 339.
- (64) Davies, C. W. *Progr. React. Kin.* **1961**, *1*, 163.
- (65) Högfeldt, E. *Stability Constants of Metal-Ion Complexes. Part A: Inorganic Ligands, IUPAC Chemical Data Series, No. 21*; Pergamon Press: New York, 1982.
- (66) Jacob, D. J.; Gottlieb, E. W.; Prather, M. J. *J. Geophys. Res.* **1989**, *94* (10), 12975.
- (67) Turco, R. P.; Whitten, R. C.; Toon, O. B. *Rev. Geophys. Space Phys.* **1982**, *20* (2), 233.